Transmission of the RGA – A Simulation with SciSim

XMM-PS-TN-38
Version 2

Christian Erd

October 2, 2000

1 Introduction

This note describes some systematics of the energy dependence of the transmission of the RGA to the EPIC beam. It is entirely based on simulations with SciSim, against which the in-flight calibrations are being compared. In this version data for the azimuthal dependence of the transmission were added together with a discussion thereof.

The key to understanding the energy dependence of the transmission function of the RGA is the overlap of the grating plates of the RGA with the exit beam per mirror shell. This is described in the next section. From this the interception of the RGA can be measured per mirror shell, which is described next. Then the results from simulations of the transmission as a function of energy are shown and discussed. Finally also the azimuthal dependence of the transmission is described.

The energy dependence of the transmission of the RGA as derived here, is stored in the CCF `RGS_QUANTUMEF`, table `RGA_OBSCURATE` (see [1, section 2.4.22] for a description).

2 Effective Area per Mirror Shell

All simulations in this section were performed for the geometry of telescope 1 (MOS1+RGS1) only. It is not important for the discussion of the qualitative explanation of the transmission function which telescope is being used.

The effective area of the mirror shells is given by the total collecting surface and by the reflectivity, which is limited in energy by the critical angle of reflection. Due to the critical angle, the efficiency of the large mirror shells is limited to low energies, where they have the largest effective area due to the larger collecting surface. This is shown in Figure 1 (solid lines), where the effective area per mirror shell is plotted for a few energies. It can be seen that at energies $> 7\,\mathrm{keV}$, the efficiency of the larger shells (lower index numbers), decreases drastically, and at very high energies (12 keV), only the smallest shells are contributing. The critical angle at 8 keV is about 30 arcmin, which is the angle of incidence on shell number 10.

The transmitted light through the RGA (dashed lines in Figure 1) to the EPIC focus shows the same qualitative contribution per mirror shell. The transmission of the RGA as a function of mirror shell is calculated as the ratio of these functions, and is plotted in Figure 2. It can be seen

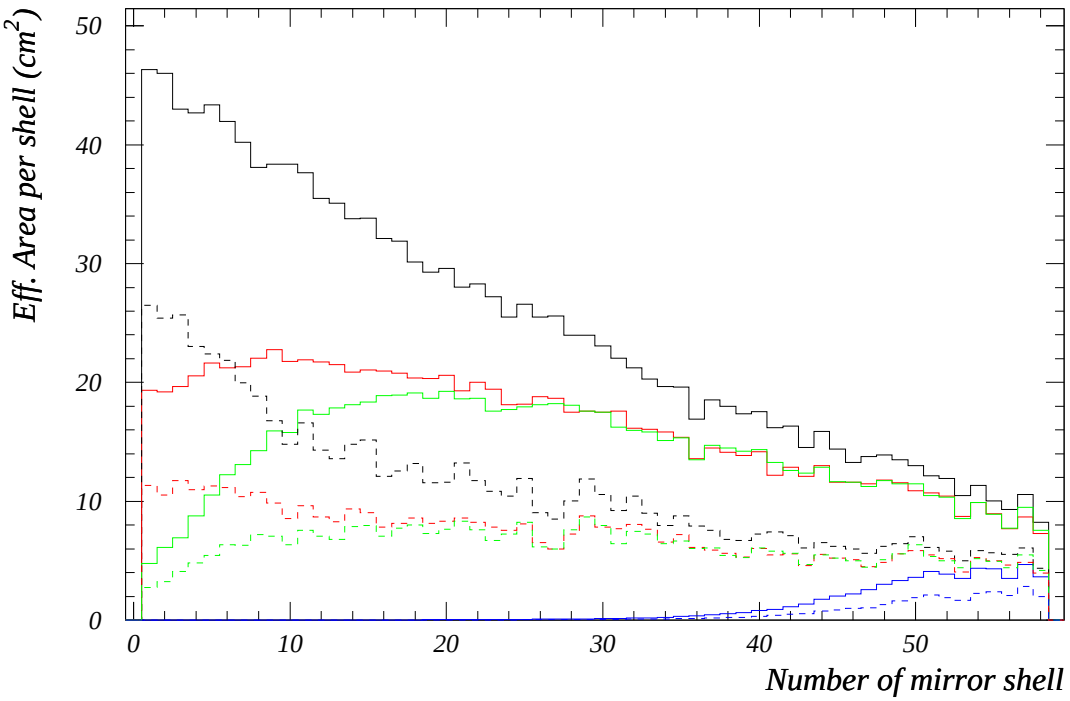

Figure 1: Effective area per mirror shell for 1 keV (black), 6 keV (red), 7 keV (green) and 12 keV (blue). Full lines are for mirror alone, dashed lines are with the RGA.

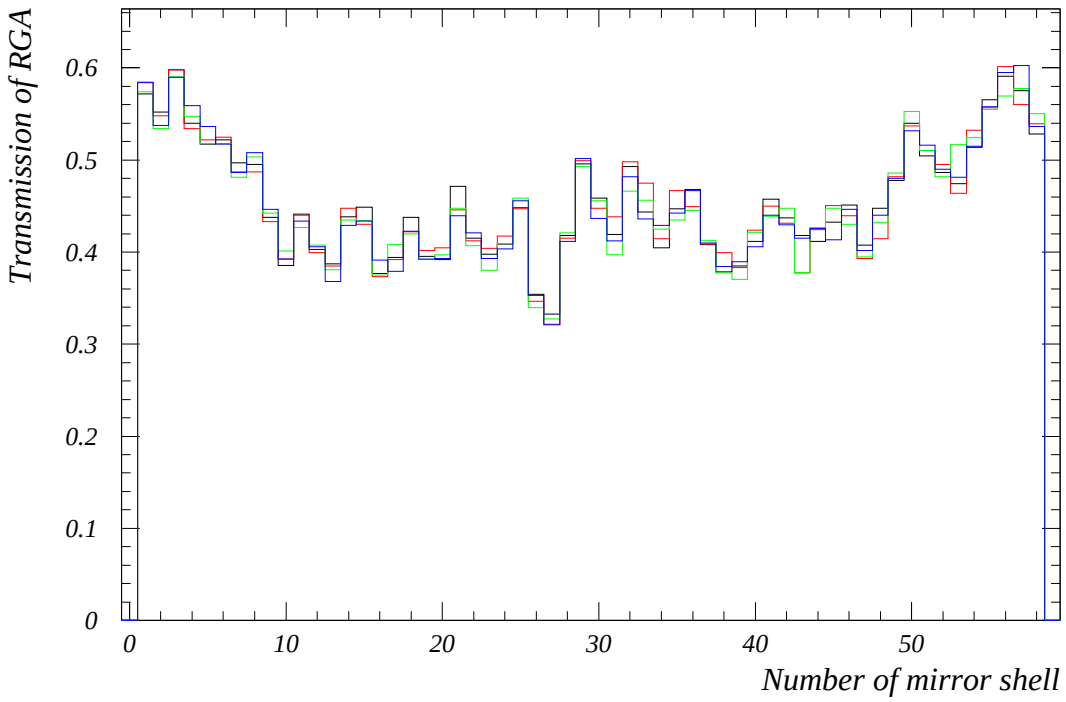

Figure 2: Transmission of RGA, calculated from the ratio of the curves in Figure 1. Color coding is the same as in Figure 1.

that there is a 20% variation from the mean value as a function of mirror shell. This is due to the alignment of the grating plates of the RGA with the exit pupils of the mirror shells. The shape of the curve can qualitatively be explained by the fact that the size of the exit pupils of the mirror shells is changing, but the spacing between the grating plates is constant.

The varying efficiency between neighboring mirror shells should be taken with caution, though, as it depends on the exact alignment of the overlap between the mirror shells and the grating plates, which is not accurately known. Minor shifts of the RGA for change the transmission from one shell to its neighbor, but we believe that the overall shape is represented correctly and has the form of higher transmission towards the inner and outer shells of the mirror, and lower transmission in the mid range.

Together with the reflectivity of the mirror shells as a function of energy, we can therefore expect a continuous reduction in transmission with increasing energy, which is due to the larger shells becoming less efficient. As the energy increases further ($>\sim$ 10 keV), only the innermost shells are collecting light, and the transmission through the RGA increases with energy.

3 Transmission as a Function of Energy

The transmission of the RGA was simulated for in-flight geometries for telescopes 1 & 2, which include MOS1+RGS1 and MOS2+RGS2, respectively. The geometry is defined in the SciSim configuration files `telescope-1.cfg` and `telescope-2.cfg`, which are part of the standard distribution of SciSim. Minor differences between the transmissions of the two RGA's are expected, because the RGA of RGS2 is mounted about 6 mm closer to the mirror than that of RGS1.

The transmission of both RGA's is shown in Figure 3 as a function of energy. The qualitative form is as expected, with a shallow decrease as a function of energy at lower energies. It also has a minimum at about 7–8 keV, and a higher transmission at high energies. This minimum occurs at energies where the shells 20–30 are becoming less efficient due to the critical angle for reflection being reached.

The transmission for energies below 4 keV is about 0.455, which matches the predictions at the ISVR very well. The minimum is only about 4% lower than this average number.

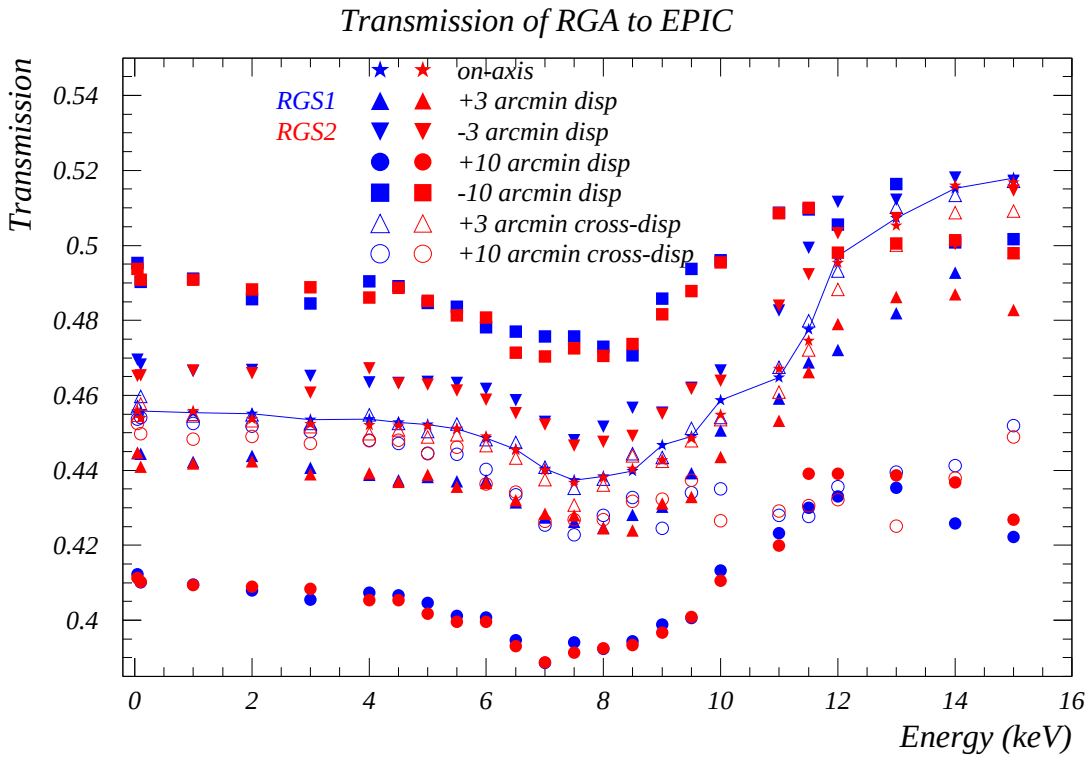

Figure 3: The transmission of the RGA as a function of energy for telescopes 1 (blue) & 2 (red). The off-axis angles are indicated in the figure. The blue line connects the on-axis transmissions of RGS1, and is drawn only to guide the eye.

4 Transmission as a Function of Off-axis Angle

For a representative subset of the energies shown in Figure 3, the transmissions as a function of off-axis angle are shown in Figure 4. Off-axis angles were investigated at two different azimuths (given in the `TELCOORD` system): parallel to the dispersion direction, at $\phi = 180°$ (blue symbols), and normal to the dispersion direction, at $\phi = 0°$ (red symbols).[1] The data are identical to those used for Figure 3, only the presentation is as a function of off-axis angle. Fewer energies were selected in order to keep the plot readable.

Although Figure 4 is produced only for one telescope, it can be seen in Figure 3 that the difference between the transmissions of the two RGS is very similar. Therefore the conclusions drawn here are applicable for both telescope systems.

4.1 Off-axis Angles Parallel to Dispersion Direction

It can be seen that the transmission is rather well behaved and according to expectations from simple geometrical arguments for the lower energy band (below the effect of the critical angle, discussed in the previous section). Along the dispersion direction, the obscuration is linear as a function of

[1] The grating plates are flat and are rotated around the Y-axis ($\phi = 90°$). For the beam to EPIC, the grating plates are acting like Venetian blinds, with a symmetric transmission for $\phi = 90°$ & $\phi = 270°$, and an asymmetric transmission for $\phi = 0°$ & $\phi = 180°$.

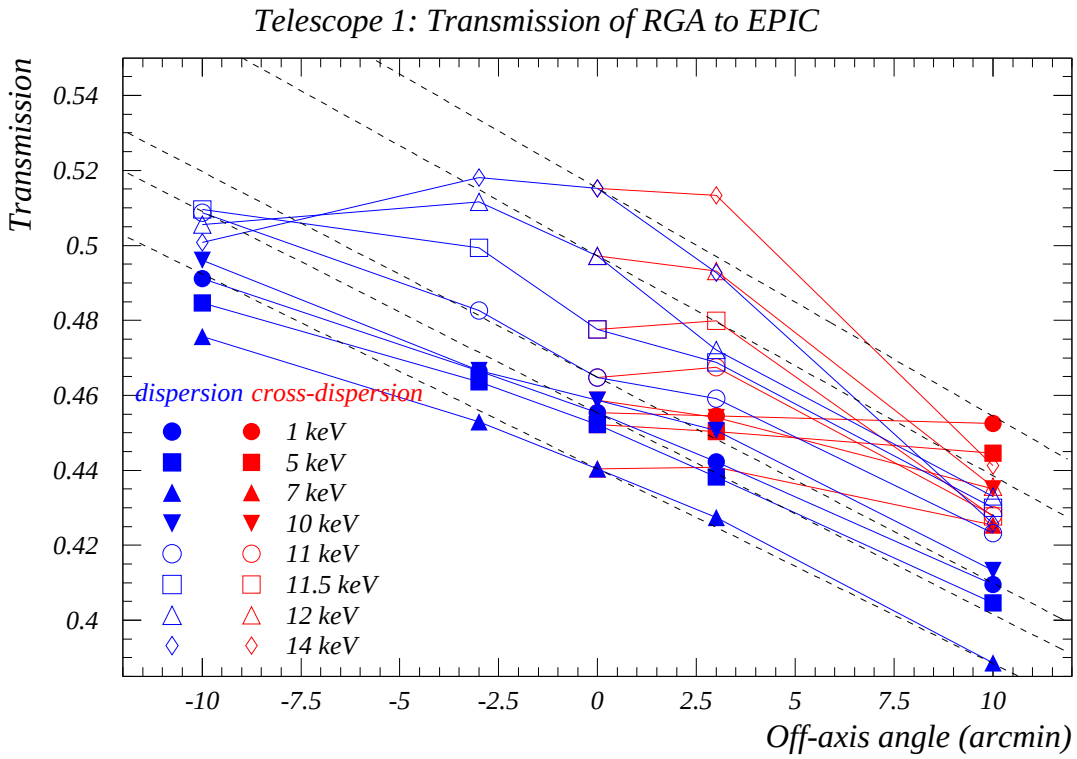

Figure 4: The transmission of the RGA for telescope 1. Blue symbols show the transmission for off-axis angles parallel to the RGS dispersion direction ($\phi = 180°$ in the `TELCOORD` reference frame), red are normal to the dispersion direction ($\phi = 90°$ in the `TELCOORD` reference frame). To guide the eye, the symbols are connected by straight lines. The parameterization that is implemented in the CAL is indicated for incident energies of 1, 7, 11, 12 and 14 keV by dashed lines.

off-axis angle. The function can be derived based on geometrical arguments from the orientation of the grating plates to the incident beam (about 1.58°). It is described in the CAL HB [1, section 2.4.22], and is also implemented in the CAL. This function is plotted by dashed lines in Figure 4. The difference between this parameterization ad the simulated transmission is 3% at ±10 arcmin off-axis angle.

For energies > 10 keV, the transmission is affected by the changing efficiency of the mirror modules due to the critical reflection angle. The smaller shells (at which the transmission of the RGA is larger) become less efficient at larger off-axis angles, because of the critical angle condition being met, and therefore the total transmission is reduced at angles of ±10 arcmin. This effect becomes most pronounced at high energies. It is not yet included in the CAL, because of lacking of in-orbit reference data, and also because it impacts in a regime where the effective area of the EPIC instruments is already reduced.

4.2 Off-axis Angles Parallel to Cross-dispersion Direction

The transmissions for source positions parallel to the cross-dispersion are shown by the red data points in Figure 4. As this is symmetric for positive and negative off-axis angles, only one component was plotted.

From the geometry of the RGA grating plates, it is expected that the transmission as a function of off-axis angle parallel to the cross-dispersion is constant. Based on these simulations this is true for energies $< 7\,\mathrm{keV}$ to 1%.

At higher energies ($> 10\,\mathrm{keV}$) and large off-axis angles ($\pm 10\,\mathrm{arcmin}$) the efficiency loss due to the critical angle reduces the transmission due to the same effect that is described before.

The current implementation in the CAL ignores this dependency and assumes a constant transmission. Again the uncertainty introduced by this simplification is largest in a regime where the response from the telescope is lowest, and due to statistical limitations of the data, a more accurate modeling is not required at this point in time.

5 Conclusions

The shape of the transmissions of each RGA was simulated with SciSim and the qualitative form of the transmission as a function of energy and a function of off-axis angle was explained. The shape of these functions is a combination of the interception of the grating plates as a function of mirror shell (Figure 1) on one hand and the loss in reflectivity of large mirror shells due to the critical angle of incidence.

The transmission has a minimum about 7–8 keV, which is only 4% lower than the average transmission at lower energies. At higher energies the transmission rises steeply and seems to flatten out at 15 keV, which is also the limit of the usable area of the mirror.

For energies $< 7\,\mathrm{keV}$ the transmission as a function of off-axis angle is according to geometrically based expectations. At higher energies the transmission falls steeper than currently modeled in the CAL.

The transmissions of the two RGA's are close to the expected values, and their functional dependences on energy and on off-axis angle are identical within the accuracy of the process. Additional systematic accuracies mainly due to uncertainties in the alignment of the RGA with respect to the mirrors are small.

The simulated values for the on-axis transmission as a function of energy (Figure 3) were included in the CCF `RGS_QUANTUMEF`. As the transmissions between the two RGA are so similar, the average values between of the two simulations were used.

This is then interpolated by the CAL for off-axis angles, which are parallel to the dispersion direction according to the function which is described in the CAL HB [1, section 2.4.22] and which is indicated by the dashed lines in Figure 4. For off-axis angles which are parallel to the cross-dispersion direction, the current implementation in the CAL is a constant function with a value of the transmission equal to the on-axis transmission. This is inappropriate for energies $> 10\,\mathrm{keV}$ and off-axis angles $> 3\,\mathrm{arcmin}$.

These functions have to be tested with in-flight calibrations of MOS data.

References

[1] Christian Erd, Phillipe Gondoin, David Lumb, Rudi Much, Uwe Lammers, and Giuseppe Vacanti. Calibration Access and Data Handbook. Technical Report XMM-PS-GM-20, issue 1.0, ESA/SSD, September 2000. http://xmm.vilspa.esa.es/calibration/docs/general/calhb.ps.gz.